Special Issue Article

Journal of Intelligent Material Systems and Structures

Journal of Intelligent Material Systems and Structures
2015, Vol. 26(13) 1622–1632
© The Author(s) 2014
Reprints and permissions:
sagepub.co.uk/journalsPermissions.nav
DOI: 10.1177/1045389X14546781
jim.sagepub.com
SAGE

Passive measurement of progressive mass change via bifurcation sensing with a multistable micromechanical system

RL Harne and KW Wang

Abstract

Mass sensing using the onset and crossing of a dynamic bifurcation of a micromechanical system has been shown to reduce the mass threshold which may be detected and exhibited improved robustness to damping and noise compared to traditional tracking of resonant frequency shift. Previous investigations demonstrated that mass measurement over time via actively controlled strategies or explored passively operated threshold-type methods to indicate a predetermined mass was adsorbed. Recently, an alternative idea integrating aspect of frequency shift- and bifurcation-based mass sensors and methods was proposed, providing initial illustration of a noteworthy ability to passively quantify progressive mass adsorption due to sequentially activated bifurcations. To advance the state of the art, this research provides a thorough investigation of this new sensing concept in terms of its dynamic characteristics and devises guidelines for effective, reliable operations. The conceptual foundation of the sensing method and an experimentally validated sensor model are reviewed. The results of numerous simulated operational trials and parametric investigations are detailed to reach important conclusions on sensor operations and versatility, and to uncover the influences of key operational conditions upon detection metrics. Finally, suitable microscale sensor architectures and fabrications are described to exemplify the flexibility of successfully realizing the mass sensing strategy.

Keywords

Mass sensing, nonlinear, bifurcation, micromechanical system

Introduction

The opportunities enabled by resonant micro/nanomechanical systems have stimulated a large body of research aimed at applications as encompassing as magnetic field detection, gyroscopic orientation, and the monitoring of mass and force changes. The latter field of study has various outlets including biological and chemical analyte detection (Thundat et al., 1995) and the probing of quantum constituents (Li et al., 2007; Schwab and Roukes, 2005). Changing mass and force in the measurement environment may be reflected by a change in the microresonator structural characteristics which thereafter induce a shift in the observed natural frequency, often the fundamental mode (Ekinci et al., 2004). The translation between shift in natural frequency and consequent monitored parameter change is ideally straightforward, but is frequently complicated by a high degree of sensitivity to noise sources and damping (Cleland, 2005; Vig and Kim, 1999), requirement for tracking hardware and interrelated resolution constraints, and difficulty to directly equate the monitored shift to the measured quantity due to response nonlinearities (Lifshitz and Cross, 2008).

To circumvent the challenges of mass detection based upon tracking the resonant frequency peak, recent studies have sought to directly utilize strongly nonlinear phenomena of microscale sensors by exploiting bifurcations. Due to the loss of stability of a given response type following small parameter change, a significant and unambiguous qualitative change in sensor response is used to denote a change in sensor mass. The ultimate limits of bifurcation-based sensing sensitivity are hinged upon thermomechanical random

Department of Mechanical Engineering, University of Michigan, Ann Arbor, MI, USA

Corresponding author:
RL Harne, Department of Mechanical Engineering, University of Michigan, Ann Arbor, MI 48109-2125, USA.
Email: rharne@umich.edu

Downloaded from jim.sagepub.com at OHIO STATE UNIVERSITY LIBRARY on July 12, 2016

motion, allowing for a theoretical detection resolution approaching individual quantum events (Zorin, 1996). For microscale mass sensing, parametric resonance (Li et al., 2014; Turner et al., 2011; Zhang and Turner, 2004, 2005) and characteristics of monostable softening Duffing oscillators (Kumar et al., 2011; Younis and Alsaleem, 2009) have been utilized to activate bifurcations. These sensors and sensing strategies have demonstrated reduced sensitivity to noise and damping compared to direct peak detection-based approaches (Turner et al., 2011; Zhang and Turner, 2004, 2005) and the opportunity to eliminate tracking hardware using one-time threshold-based switches (Kumar et al., 2011; Younis and Alsaleem, 2009). Yet challenges still remain including an inability to passively control the probability distribution of triggering thresholds encountered during mass accumulation sweeps, potential for adverse nonlinear phenomena encountered with prolonged excitation approaching a bifurcation frequency (Baesens, 1991; Berglund and Gentz, 2000; Lu and Evan-Iwanowski, 1994) which inhibits reliable detection, and mass *measurement over time* relies on additional active hardware. These initial explorations of bifurcation-based mass sensing indicate great promise, but much remains to be uncovered and improved upon to fully capitalize on the potential.

To address the existing limitations and enhance sensor versatility, the authors recently introduced an alternative sensor platform and corresponding sensing strategies that integrate aspects of frequency shift-based and bifurcation-based mass sensors and methods (Harne and Wang, 2014). The mass sensing strategies included a *passive* approach and a *controlled* frequency sweeping approach, each providing important service and functionality. A model of the sensor platform was formulated and validated by experimentation with a proof-of-concept device. By combination of sensor development and sensing strategy, the ability to *passively* quantify mass adsorption over time was initially illustrated. It was conceptually stated that, by the passive mass measurement approach, one can tailor the system to address application constraints and meet preferred detection sensitivities. However, in the scope of the past research, the *passive* mass measurement ability was presented only via the fundamental illustrations and not explored to further depth. Numerous experimental investigations using the *controlled* frequency sweeping strategy exemplified its robustness for accurate detection of accumulating mass as compared to tracking the shifting resonance frequency peak. Finally, using a stochastic model, insight into the influences of additive noise interferences on the first jump events was provided through direct numerical simulations to assess non-deterministic sensitivities of the sensing methods.

From the initial evidence and conceptual foundation (Harne and Wang, 2014), it is clear that a significant advancement in ease of implementation for microscale mass sensing may be realized via the proposed sensor and sensing strategy that enable *passive* measurement of progressive mass adsorption. However, apart from the broad methodology overview and first example demonstrating its feasibility in the authors' prior study, the potential of the passive mass sensing approach remains otherwise unexplored. Indeed, critical factors influencing the passive mass measurement strategy in its ideal, deterministic operation—including operational parameter influences, initial condition sensitivities, and preferred employment schemes and guidelines—were not evaluated in the prior research. Therefore, to advance the understanding and realizable achievement of the new mass measurement approach, the aims of this research are to provide a thorough investigation of its characteristics, explore the method's operational sensitivities, and to devise guidelines for its effective and reliable implementation.

In this paper, a brief review of the proposed sensor platform, the passive operational strategy, and their modeling is first presented. These include the key rationales dictating architecture and sensing strategy development, which are necessary background information to clarify prior to presentation and discussion of the new investigations. Then, the results of numerous sensing trial simulations are evaluated to uncover key trends regarding mass detection sensitivity and trial repeatability with the passive mass measurement approach. A wide range of operational conditions and design parameters are considered to thoroughly probe the sensor and method. From the parametric studies, useful implementation guidelines are presented for ensuring the system's effectiveness and reliability to passively measure mass adsorption over time. Finally, to complement this article's focus on sensing *strategy*, discussion is provided on several potential sensor *architecture* designs and fabrication protocols to successfully realize the system on the microscale.

Rationale for sensor architecture and sensing strategy

In this section, for the sake of completeness, a review of the new sensor platform and passive mass measurement strategy is provided to summarize the conceptual foundation developed in the previous study (Harne and Wang, 2014). As compared to existing bifurcation-based sensing strategies that use mass adsorption to shift a bifurcation *frequency* such that it coincides with the excitation frequency, the proposed system uniquely leads to an excitation *level* sweep for the bifurcating component. The change in effective sweeping style enables a critical ability to activate bifurcations in sequence for passive measurement of progressive accumulation of mass on the sensor. Although only conceptually described in the previous work, as will be

Downloaded from jim.sagepub.com at OHIO STATE UNIVERSITY LIBRARY on July 12, 2016

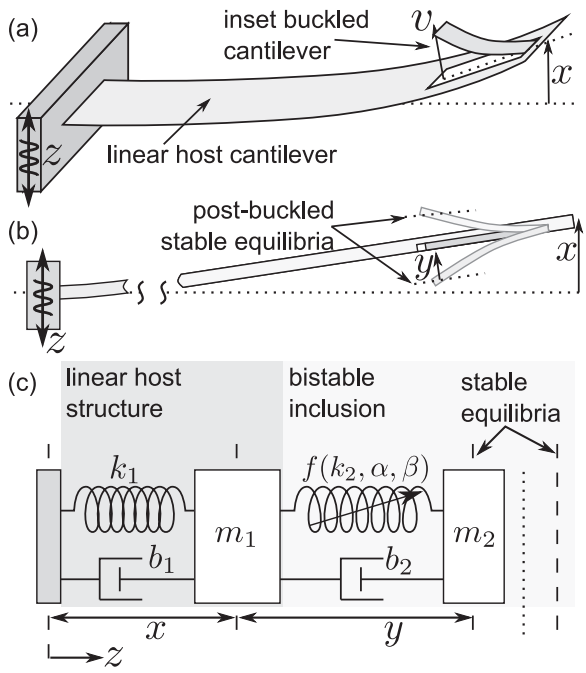

Figure 1. Schematic of coupled linear–bistable micromechanical sensor architecture as adapted and redrawn in the style of (Harne and Wang, 2014): (a) realization via host microcantilever and inset buckled cantilever, (b) schematic showing coordinate convention used in model, and (c) lumped parameter representation of (b).

apparent in the later detailed discussions of the findings of this research, the sensor and method may be favorably employed to strategically govern the manner and rate of triggering the bifurcations. This helps to directly tailor the probability distribution of jump events, and therefore the detection reliability, regardless of mass accumulation rate.

To achieve this flexibility of operation, the sensor architecture is a 2-degree-of-freedom (DOF) system where the excited element is a host linear resonator upon or into which is attached a small, bistable nonlinear inclusion. In the sensor embodiment shown in Figure 1(a), the host resonator is an excited microcantilever having a buckled inset beam at the host beam free end. In the authors' recent study, the inset bistable beam of a sensor prototype was buckled via repulsive magnetic forces (Harne and Wang, 2014). Alternative coupled linear–bistable sensor realizations may be envisioned, and greater details regarding suitable microscale platforms and fabrication methods are given in the final section of this paper. However, the essential components of design require that the host be significantly more massive than the small bistable inclusion and that the linear natural frequency of the bistable inclusion be much greater than the host structure natural frequency such that the second linear mode natural frequency of the coupled system is much greater than the fundamental mode resonance.

In contrast to parametric resonators or softening Duffing oscillators employed by the past studies, a *bistable* element is selected as the strongly nonlinear component due to an increased assurance of bifurcations across large range of damping level (Kovacic and Brennan, 2011) and the opportunity to utilize the critical events sequentially. The advantage of the 2-DOF sensor platform is the dynamic coupling between the host linear resonator and smaller bistable inclusion, which serves to crucially transform mass adsorption upon the host into an *effective excitation level sweep* for the bistable inclusion. Such an effective sweep for the bistable inclusion is necessary to enable sequential activation of bifurcations for passive measurement of adsorbed mass over time, that is, when the whole sensor is driven by unchanging excitations like the base excitation in Figure 1(a).

The ability to passively activate sequential bifurcations in consequence to steady mass adsorption was recently demonstrated by direct numerical simulation using a coupled linear–bistable sensor architecture for microscale mass sensing (Harne and Wang, 2014) and by experimentation with a coupled mechanical–electrical oscillator system for structural monitoring applications (Harne and Wang, 2013). To achieve this unique sensing functionality, the sensor excitation is driven at a constant frequency that is less than the fundamental mode natural frequency prior to mass accumulation. The sensor excitation level is selected such that the bistable inclusion initially oscillates with small amplitude intrawell oscillations around one of the stable equilibria. Because the operational strategy only concerns the bandwidth immediately around the fundamental mode, both bodies of the 2-DOF sensor vibrate in phase. Thus, from the perspective of the small bistable inclusion, the influence of the base excitation level and host oscillation is comparable to a *variable gain excitation source*. The sensor initialization point is represented by point 1 in Figure 2, showing the fundamental mode response transfer function amplitude, $H = \{[k - \omega^2 m(t)]^2 + [\omega b]^2\}^{-1/2}$, as a function of excitation frequency ω and increasing modal mass $m(t) = m + \delta m(t)$ due to accumulating mass $\delta m(t)$. The red solid curve in Figure 2 is therefore representative of the excitation level up and down sweep for the bistable inclusion induced via steady mass accumulation on the sensor.

As mass adsorbs on the larger host resonator, the effect is to reduce the fundamental natural frequency, thus gradually amplifying sensor response levels because the resonance approaches the constant sensor excitation frequency. Eventually, a time is reached at which the amplified level is great enough to trigger the bifurcation of the bistable inclusion that activates the unmistakable switch from low amplitude intrawell to high amplitude interwell vibrations, represented by point 2 in Figure 2. The fine degree of mass adsorption

Downloaded from jim.sagepub.com at OHIO STATE UNIVERSITY LIBRARY on July 12, 2016

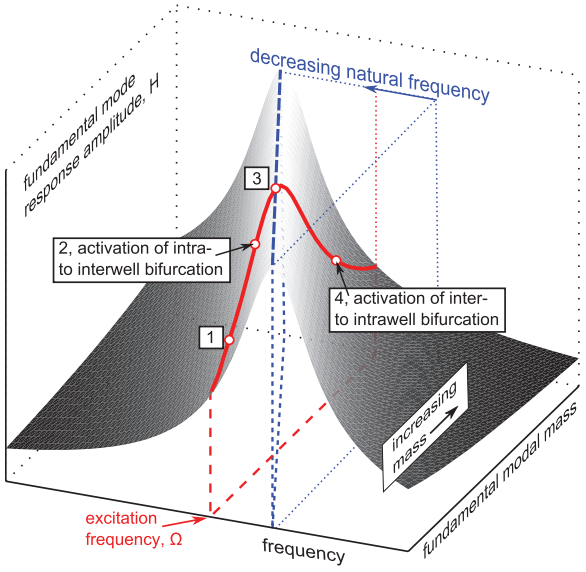

Figure 2. Concept of sequential bifurcation activation in consequence to fundamental mode response transfer function amplitude shifting due to mass adsorbing over time, adapted and redrawn in the style of Harne and Wang (2014). At a constant excitation frequency, the response amplitude H changes because the natural frequency reduces due to progressive mass accumulation. Thus, at constant excitation frequency, the sensor response is amplified to varying levels depending on the amount of adsorbed mass.

necessary to push the bistable element across the critical point is the trademark of high sensitivity bifurcation-based mass sensing. However, further steady mass accumulation on the sensor may still be monitored by the proposed 2-DOF system. Continuing with the example, eventually mass adsorption reaches the level that the reduced fundamental natural frequency coincides with the excitation frequency, and effective amplification gain to the bistable inclusion is maximized, as in point 3 in Figure 2. Thereafter, further mass accumulation indicates the system is excited above resonance and thus reduces the effective excitation level working on the bistable element, leading to the bifurcation drop down in response amplitude (inter- to intrawell oscillations), as in point 4. Conceptually, the sequential activation of bifurcations is straightforward when considering the influence of the varying fundamental mode response amplitude as an effective excitation level sweep up and then down for the bistable inclusion. Such dynamic influence is comparable to recent vibration energy harvesting studies that investigated the addition of "dynamic magnifier" resonators to amplify external excitation levels to enhance energy harvesting performance for the attached electromechanical oscillators (Aldraihem and Baz, 2011; Wu et al., 2012; Wu et al., 2014; Zhou et al., 2012). In the sensing context, two bifurcation events observed in sequence are needed to quantify mass over time in a passive manner as will be detailed in a later section of this paper. This ability notably contrasts previous bifurcation-based microscale mass sensing studies that used actively controlled strategies to measure progressive mass accumulation (Zhang and Turner, 2005) or employed passive methods that only indicate a threshold amount of mass was adsorbed (Kumar et al., 2011; Younis and Alsaleem, 2009). To best capture the importance of the novel utility enabled by the proposed sensor, a model of the sensor architecture was developed and validated (Harne and Wang, 2014). The model formulation is reviewed in the next section.

Modeling and governing equations

The governing equations of the sensor platform are derived according to lumped parameter assumptions, which are appropriate in light of the intended operation around the fundamental mode resonance and the principal vibration response of many micromechanical systems (Lifshitz and Cross, 2008). The sensor system is shown in Figure 1(a) indicating the host structure displacement relative to base motion, x, and the relative displacement between the bistable element and host structure, v, as the response coordinates. The governing equations of the lumped parameter system are derived as

$$m_1(\ddot{x} + \ddot{z}) + b_1\dot{x} + k_1 x - b_2\dot{v} - \Lambda'(v) = 0 \qquad (1a)$$

$$m_2(\ddot{v} + \ddot{x} + \ddot{z}) + b_2\dot{v} + \Lambda'(v) = 0 \qquad (1b)$$

where m_i, b_i, and k_i are effective mass, damping, and linear stiffnesses of the sub-systems, respectively, and $i = 1,2$; $\Lambda(v)$ is the potential energy of the bistable element as function of relative displacement coordinate v; and operators $(\dot{\cdot})$ and $(\,)'$ denote time and spatial derivatives, respectively. In this study, the double-well potential energy profile is utilized for the bistable inclusion which represents a variety of microscale bistable system potentials when considering fundamental buckling mode response (Harne and Wang, 2014; Krylov et al., 2011; Ruzziconi et al., 2013)

$$\Lambda(v) = -\frac{1}{2}k_{2L}v^2 + \frac{1}{4}k_{2NL}v^4 \qquad (2)$$

The spatial derivative of the potential energy, $\Lambda' = \partial\Lambda/\partial v$, is the restoring force from which may be computed the fixed points of the bistable sub-system: $\Lambda'(v) = 0 \rightarrow v^* = \pm\sqrt{k_{2L}/k_{2NL}}$. Here, v^* are the stable equilibria that are symmetric with respect to a central unstable configuration. A coordinate transformation is then applied by defining $y = v - v^*$ such that the bistable inclusion response coordinate y is 0 at one of the stable positions, as indicated in schematics of Figure 1(b) and (c). Substitution of the transformation

Downloaded from jim.sagepub.com at OHIO STATE UNIVERSITY LIBRARY on July 12, 2016

into equation system (1) and following simplification leads to equation system (3)

$$m_1\ddot{x} + b_1\dot{x} + k_1x - b_2\dot{y} - k_2y[1 + \alpha y + \beta y^2] = -m_1\ddot{z} \tag{3a}$$

$$m_2\ddot{y} + (1 + (m_2/m_1))[b_2\dot{y} + k_2y(1 + \alpha y + \beta y^2)] - \left(\frac{m_2}{m_1}\right)(b_1\dot{x} + k_1x) = 0 \tag{3b}$$

Here, $k_2 = 2k_{2L}$, while $\alpha = 3\sqrt{k_{2NL}/k_{2L}}$ and $\beta = k_{2NL}/k_{2L}$ are stiffness proportionality constants, and $-\ddot{z} = Z_a \sin \Omega t$ is the harmonic base acceleration of amplitude Z_a and frequency Ω. In the event of practical and oftentimes unavoidable bistable inclusion asymmetries (Harne and Wang, 2014; Krylov et al., 2011; Ruzziconi et al., 2013), proportionality constants α and β may be modified from the prior definitions such that the equilibria are positioned at $v^* = [-\alpha \pm \sqrt{\alpha^2 - 4\beta}]/2\beta$ and at $v^* = 0$.

Having reviewed the sensor platform composition, the dynamic concept behind the passive sensing strategy, and the modeling formulation, the following sections present the new investigations performed to advance the understanding of the proposed passive mass measurement system through explorations of its sensitivities. From these new insights, preferred design and implementation guidelines may be devised, which assist in latter discussions regarding realizable sensor architecture fabrications.

System operation studies

In this section, simulated demonstrations of the sensor implementation are provided to observe key operational parameter influences and overall functionalities. In the following simulations, for simplicity it is assumed that mass is adsorbed only upon the larger host structure such that the time-varying mass of the host is $\bar{m}_1(t) = m_1 + \delta m(t)$. Figure 3 plots computed velocity responses for various constant excitation conditions as mass accumulates at a linear rate of 0.001 mass ratio (mr) per second, where mr is the ratio of adsorbed mass $\delta m(t)$ to primary linear structure mass m_1. The results are calculated by numerically integrating equation system (3) in MATLAB. Simulations in rows (a, b) and (c, d) are conducted using base acceleration levels of 5 and 7 m/s^2, respectively. In column (a, c), the system is excited at 99.4% of the baseline fundamental mode natural frequency f_1 prior to mass accumulation, while in column (b, d) the excitation frequency is 99.5% of f_1. Other parameters used in simulation are given in Table 1.

The unique elements and dynamic sensing events described conceptually earlier in this work are all evident in the simulation results shown in Figure 3: progressive amplification and then reduction in sensor response due to the fundamental resonance shifting downward in frequency because of mass adsorption, the activation of a low-to-high amplitude (intra- to interwell) response bifurcation for the bistable inclusion, and the later activation of an inter-to-intrawell bifurcation down in amplitude. When the high amplitude response is activated, there is a sudden and apparent increase in bistable inclusion velocity. During the period when the energetic oscillations are activated, both DOF of the sensor exhibit highly perturbed responses due to the strongly nonlinear interwell vibrations of the bistable inclusion. In comparing Figure 3(a) to (b) and (c) to (d), change in constant excitation frequency is seen to primarily shift the points in time at which the bifurcations occur but does not notably change the span of time elapsed between jumps. In contrast, changing overall sensor excitation level Z_a, as shown comparing Figure 3(a) to (c) and (b) to (d), reveals that the span of time between jumps is adjusted; specifically, as level increases, the time elapsed between bifurcations increases, and vice versa.

Because two bifurcation events occur in sequence, net mass accumulation may be determined using knowledge of time elapsed between jumps and the known mass accumulation rate. In Figure 3, these quantities are provided as Δmr values. Outside of controlled laboratory experimentation, accumulation rate would likely be unknown, and thus a bifurcation analysis of equation system (3) is needed to derive closed-form expressions for the critical mass quantities required, using a given excitation parameter set, to activate each bifurcation event. Comparable bifurcation analyses were utilized by prior bifurcation-based sensing studies for mass detection (Zhang et al., 2003; Zhang and Turner, 2005) as well as force measurement (Hassanpour et al., 2011) to determine expressions related to their representative sensor architectures. Likewise, for the present sensor platform, such analysis represents a 2-DOF example of the 1-DOF derivation conducted in a prior study by the authors in the context of vibration energy harvesting with bistable systems (Harne et al., 2013). With derived expressions for the critical mass values to induce the bifurcations, the occurrence of both jumps in sequence *passively indicates* an amount of mass was adsorbed in the span of time which elapsed such that both bifurcations were triggered. As shown in studying trends of Figure 3, selection of constant excitation *frequency* is the means to control the initial nearness to bifurcation (and hence the ultimate sensitivity to a pre-determined change in sensor mass), while the constant sensor excitation *level* tailors the time elapsed between jumps (and hence the amount of mass that is measured). Since the excitation conditions are selected by the user or designer of the sensor, these critical mass sensing factors may be directly adjusted for the specific application of interest. These insights were not obtainable through the investigations of the past study by Harne and Wang (2014)

Downloaded from jim.sagepub.com at OHIO STATE UNIVERSITY LIBRARY on July 12, 2016

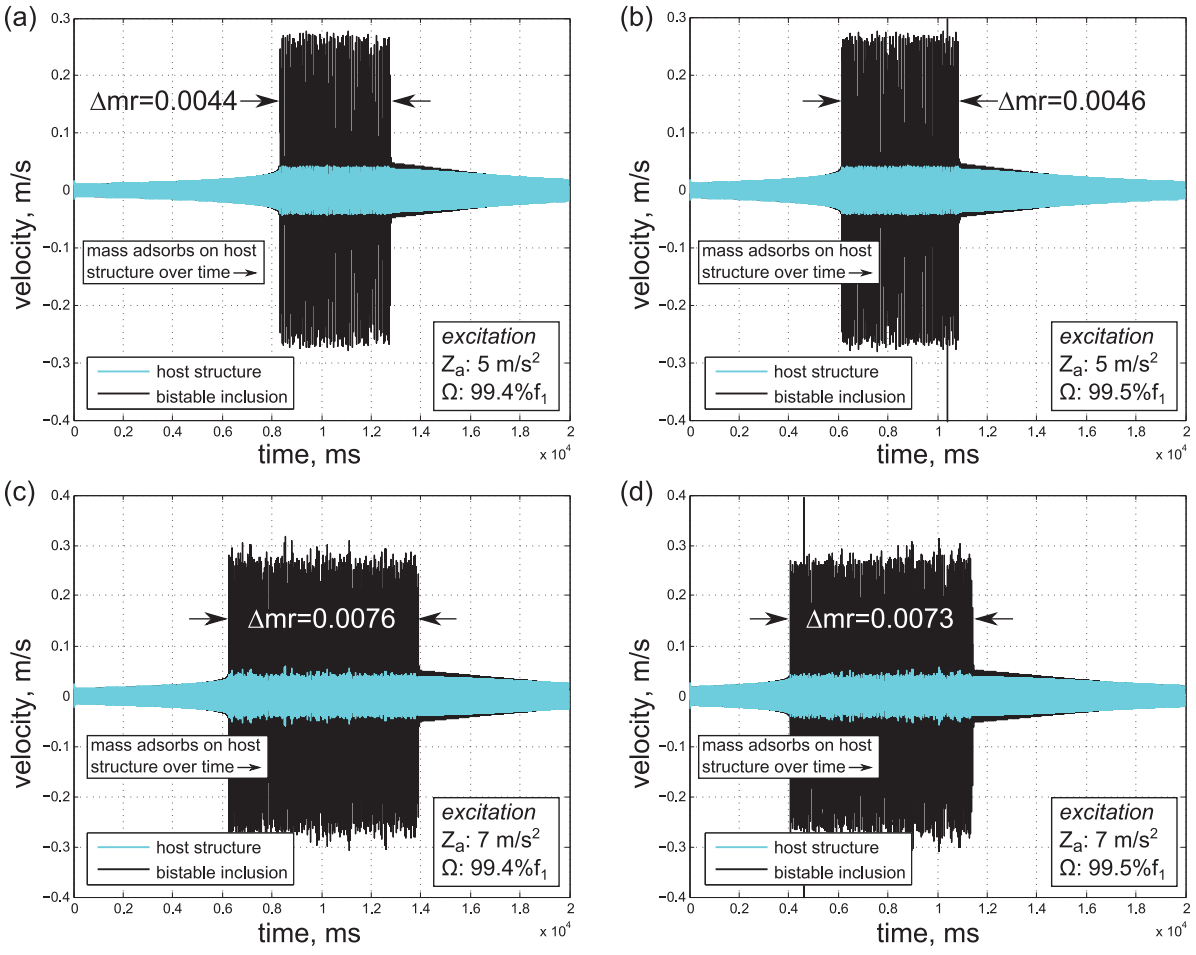

Figure 3. Velocity responses due to steadily increasing mass accumulation upon sensor host structure with excitation at (a, c) 99.4% of the baseline fundamental mode resonance f_1 prior to mass accumulation, and (b, d) 99.5% of f_1. Row (a, b) at Z_a = 5 m/s^2 base acceleration level, and row (c, d) at Z_a = 7 m/s^2.

Table 1. Simulation parameters.

m_1 (ng)	m_2 (ng)	b_1 (nN s/m)	b_2 (nN s/m)
5	0.1	471	18.2
k_1 (N/m)	k_2 (N/m)	α (1/m)	β (1/m^2)
7.11	0.299	4.57×10^5	4.64×10^{10}

and suggest further comprehensive explorations may uncover additional critical abilities and sensitivities of the passive mass measurement strategy that may lead to the development of valuable design guidelines.

Investigations of operational parameter influences

Observations from the examples in Figure 3 suggest general trends related to changing sensor excitation frequency and level. However, a more deliberate assessment is required to develop well-supported conclusions regarding such dependencies and to determine useful guidelines for effective passive measurements of progressive mass adsorption. To achieve these objectives, the following studies assess the critical influences of excitation conditions in addition to the accumulation rate of the monitored analyte mass.

Sensor excitation frequency and level

Figure 4 presents results of changing the constant excitation frequency in terms of the final amount of added mass ratio that is measured, for a wide range of sensor excitation levels and fixed mass ratio adsorption rate of 0.001. The minimum excitation level was selected to ensure that sequential bifurcations were activated in all simulated trials. Each data point represents the mean absorbed mass ratio value determined from 40 simulated trials, while bars are first standard deviations. Random initial conditions are employed for each trial. Both trends observed in Figure 3 regarding constant excitation frequency and level are consistently supported throughout the results of Figure 4. Change in

Downloaded from jim.sagepub.com at OHIO STATE UNIVERSITY LIBRARY on July 12, 2016

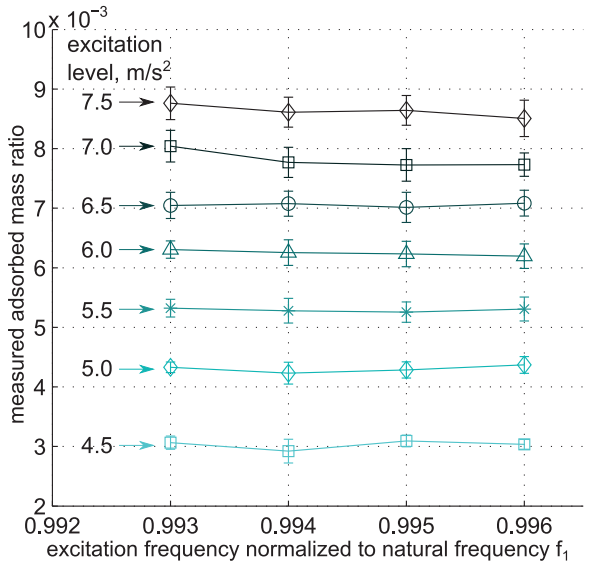

Figure 4. Measured adsorbed mass ratio as function of constant excitation frequency and level. Mass ratio accumulation rate for all trials is 0.001. Data points are mean values across 40 simulated trials; bars are first standard deviations.

excitation frequency has little influence in modifying the amount of added mass measured, whereas the excitation level plays a clear role in adjusting the value. However, the results show deviation around a mean value, and the adsorbed mass amount is not entirely insensitive to change in excitation frequency.

These findings reflect the initial condition dependence of strongly nonlinear systems and the non-stationarity of the system (mass changing over time), which lead to non-uniform activation of the bifurcations from trial to trial. The deviation around mean adsorbed mass values is seen to increase as the excitation level increases. This result is intuitive when considering the conceptual framework of activating the bifurcations using the 2-DOF sensor architecture. As illustrated in Figure 2, the shifting fundamental resonance leads to amplification and then reduction in the sensor response at a fixed excitation frequency. Since mass accumulates at a linear rate in the simulated trials, every time instant corresponds to a specific value of $\partial H/\partial m$ according to the slope of the fundamental mode resonance, as shown in Figure 2. By increasing sensor excitation levels, the representative bifurcation points 2 and 4 in Figure 2 effectively move down the surface contour, which means that smaller rates $\partial H/\partial m$ activate the critical events. Because prolonged steady-state oscillation close to a bifurcation may lead to spurious switching events due to the initial condition sensitivity of strongly nonlinear systems (Baesens, 1991; Berglund and Gentz, 2000; Lu and Evan-Iwanowski, 1994) and because the saddle-node bifurcation here utilized may exhibit fractal basin of attraction erosion as the system passes through bifurcation (Soliman and Thompson, 1989), the "shallower" slopes $\partial H/\partial m$ caused by too high of excitation levels are not conducive to repeatable triggering. Thus, Figure 4 shows that increasing excitation level produces larger deviations of quantified mass value as compared to the smaller excitation levels which take advantage of the "steeper" slopes of the shifting fundamental resonance to more reliably activate bifurcations from the same increment of adsorbed mass over time. This finding indicates a clear means to directly ensure that the sensing strategy maintains viability by modification of the sensor excitation level. This is a versatility for passive bifurcation-based microscale mass sensing otherwise achieved only by employing actively controlled approaches to date (Burgner et al., 2010).

Mass adsorption rate

Because mass accumulates at a finite rate in practical mass sensing contexts, the sensor response is non-stationary. This factor is important because the specific parameters of periodic non-stationary excitations have a strong influence on the outcomes of *both* nonlinear and linear system responses (Cronin, 1966; Lewis, 1932; Lu and Evan-Iwanowski, 1994). Consequently, sensor sensitivity to change in adsorption rate must be characterized for important design and operating guidelines. Change in adsorption rate represents practical microscale mass sensing scenarios such as rapid diffusion of a noxious gas or slow particle accumulation to evaluate ultimate detection sensitivity in the laboratory. Thus, a wide range of rates should be considered to thoroughly assess the proposed sensor architecture and sensing strategy.

Figure 5 plots results of the measured adsorbed mass ratio as function of the accumulation rate. Each data point is the mean value for a given excitation level computed from 40 simulated trials across a range of five excitation frequencies: thus each data point is the mean from the results of 200 simulations. The bars are first standard deviations. Ideally, variation in adsorption rate should not influence the ultimate amount of mass that accumulates on the sensor spanning the sequential bifurcations. However, Figure 5 indicates that across the range of excitation levels, there is some degree of sensitivity to adsorption rate changes. In general, the faster the rates, the greater the deviation of results. These trends become more apparent for increased excitation levels. Non-stationary passage through bifurcation is a process prone to variability, but as higher excitation levels drive the sensor to greater degrees of strongly nonlinear response, the sensitivity to the ultimate point at which the bifurcations occur is likewise heightened. The trend for higher excitation levels and faster adsorption rates is an increase in the adsorbed mass that is measured. Recall that from the perspective

Downloaded from jim.sagepub.com at OHIO STATE UNIVERSITY LIBRARY on July 12, 2016

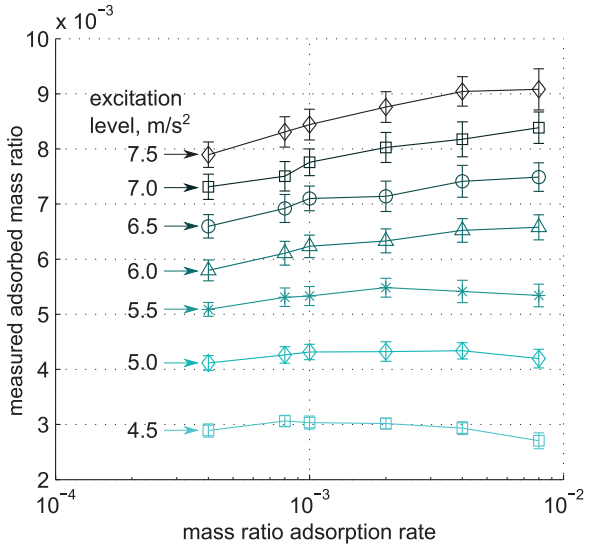

Figure 5. Measured adsorbed mass ratio as function of mass ratio adsorption rate and excitation level. Data points are mean values across five sets of excitation frequency each using 40 simulated trials; bars are first standard deviations.

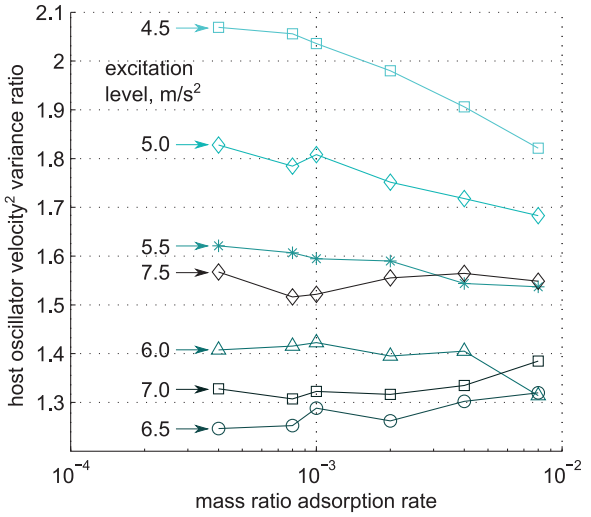

Figure 6. Ratio of host oscillator velocity^2 $|\dot{x}|^2$ variance during energetic response period to before/after as function of mass ratio adsorption rate and excitation level. Data points are mean values across five sets of excitation frequency each using 40 simulated trials.

of the small bistable inclusion, the effect of mass accumulation is like an effective excitation level sweep up and down to sequentially induce the bistable element bifurcations. The prior trend of increasing measured mass as excitation level and absorption rate both increase is explained because the bifurcation drop downward from inter- to intrawell oscillations is more sensitive to initial conditions during non-stationary excitation level sweeps, leading to *delayed* or *deferred* bifurcations, than is the opposite bifurcation upward in response amplitude (Lu and Evan-Iwanowski, 1994). Thus, results of Figure 5 reveal that for the highest excitation levels, the sensor remains activated in the interwell response for too long and consequently quantifies an erroneous increasing amount of accumulated mass. Uncovering these important trends helps to determine sensor excitation levels desirable to minimize adverse influence of non-stationarity on the reliability of the passive mass measurement strategy.

Feasibility of detection

A final evaluation is valuable in light of sensor data readout constraints. Depending on the fabrication process selected for the microscale sensor, it could be challenging to electrically isolate the bistable inclusion from the host so as to strictly measure the response of the smaller inclusion. Thus, it may be necessary to rely on response measurements acquired solely from the host resonator. Therefore, this section evaluates the feasibility of monitoring only the host linear resonator velocity response, which, it is assumed, will be measured via one of many common transduction methods proportional to velocity, for example, optical, piezoresistivity, etc. Specifically, the metric of performance used here is the ratio of variance of the host structure squared velocity *during* the energetic interwell vibration period to that measured *before and after* the jumps (the intrawell oscillations). Thus, larger values of this metric indicate that detection of the bifurcation events is more easily observed.

Figure 6 presents results of the mean values of variance ratio determined from five constant excitation frequencies using 40 simulated runs each, across a range of excitation levels and mass adsorption rates. The results show an undesired variance ratio minimization for excitation level of 6.5 m/s^2, an explanation of which is not immediately apparent. However, more importantly, the smaller excitation levels yield the greatest variance ratios beneficial for bifurcation detection, particularly for the slower mass ratio adsorption rates. The variance ratios for the smaller excitation levels reduce as mass adsorption rate increases but still remain greater than that provided by higher excitation levels.

Recalling that the smallest excitation level in the simulated studies was selected because it ensured that both bifurcations were activated at some point during the sensing trials, the results of Figures 4 to 6 suggest that the smallest excitation level usable to activate both jump events is the most beneficial for the proposed sensor architecture and sensing strategy. Through the parametric investigations, it is seen that the smallest excitation level (a) leads to the least deviation around the mean value for the amount of adsorbed mass that

Downloaded from jim.sagepub.com at OHIO STATE UNIVERSITY LIBRARY on July 12, 2016

is measured, (b) shows reduced sensitivity to adverse change in measured mass as accumulation rate changes, and moreover (c) leads to the most useful host linear resonator variance ratio for mass detection from the more easily acquired measurements of the larger host resonator. The results, therefore, set valuable guidelines for implementation of the proposed sensor to ensure its operation remains effective and reliable.

Sensor embodiments and fabrication strategies

The coupled linear–bistable sensor in Figure 1(a) was realized on the mesoscale by the authors to provide experimental proof-of-concept demonstrations and model validations (Harne and Wang, 2014). While the primary aims of this study have been to thoroughly investigate the passive mass sensing *strategy* and devise guidelines for its effective and reliable operation, it is valuable to provide complementary discussion on microscale sensor *embodiments* and fabrication methods that may be employed to satisfy the general architecture requirements.

Developments in two fields—atomic force microscopy (AFM) and vibration energy harvesting—together demonstrate a suite of opportunities to realize the coupled linear–bistable sensor platform shown in Figure 1(a) using coupled microcantilevers. With the aims of enhancing AFM sensitivity and topographical reconstruction resolution, microcantilever-in-cantilever sensors have been fabricated where the oscillator inclusions have been machined facing, opposing, and orthogonal to the free end of the host cantilever (Loganathan and Bristow, 2014; Sarioglu et al., 2012; Shaik et al., 2014). Such designs would meet the elastic and geometric requirements of the proposed linear–bistable sensor in Figure 1(a), but magnet deposition would also be needed to induce bistability. Recent studies in vibration energy harvesting using energetic bistable systems have provided detailed fabrication protocols and demonstrated successful deposition of repulsive permanent magnets on microcantilever ends (Andò et al., 2010; Emery, 2014). Together, these sensor designs and fabrication methods meet the architecture requirements of the proposed sensor in Figure 1(a).

Alternative sensor platforms may be envisioned, which satisfy the coupled linear–bistable design framework. For example, Figure 7 is a schematic for coupled in-plane oscillators, where an electrostatically actuated host oscillator contains an inset curved beam, and thus, bistability is realized by the geometry itself rather than electrostatic, magnetic, or otherwise multi-physics interactions. Such configuration would employ comparable etching procedures as a recently realized large-stroke actuator, which in fact utilized serially connected bistable curved beams with an inset, actuated mass (Gerson et al., 2012). In spite of the opposite configurational order, the success of fabricating microscale, serially connected linear and bistable in-plane oscillators supports the feasibility of the proposed schematic in Figure 7. Moreover, by utilization of a geometrically bistable inclusion—that is, bistability by mechanics—one may alleviate intricate coupling concerns related to achieving bistability via electromechanical factors (Abu-Salih and Elata, 2006; Elata and Abu-Salih, 2005; Hassanpour et al., 2011) or other multi-physics methods generally. These examples provide evidence that successfully realizing the passive mass sensing strategy on the microscale is not constrained to one specific sensor architecture and may be employed according to fabrication expertise and packaging preferences, be they for out-of-plane cantilever vibrations or in-plane shuttle oscillator dynamics.

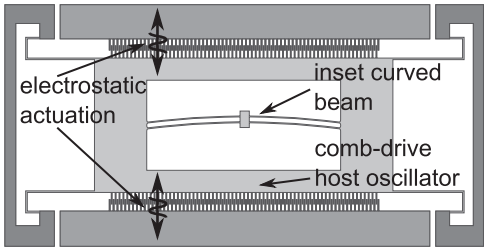

Figure 7. Schematic of coupled linear–bistable sensor architecture employing in-plane dynamics of electrostatically actuated, host comb-drive shuttle oscillator and inset curved beam.

Conclusion

A 2-DOF sensor architecture and sensing strategy have been proposed to advance the performance and versatility of microscale bifurcation-based mass sensing. Together, the sensor and sensing approach exploit the sequential activation of a bistable element's bifurcations, thus enabling a novel ability to passively measure adsorbed mass over time. The research reported in this paper provides a thorough investigation of this important ability and devises guidelines for its effective and reliable operation. Through the studies, it is found that the sensor and sensing strategy provide unique means to adjust critical sensor sensitivities for maintaining measurement consistency regardless of mass adsorption rate. By tailoring operating conditions, the specific amount of accumulated mass measured over time may be directly adjusted and effective sensor readout using only the larger host structure may be ensured. Moreover, the sensor architecture requirements are met by multiple platform designs, exemplifying flexibility in implementing the sensing strategy based upon

Downloaded from jim.sagepub.com at OHIO STATE UNIVERSITY LIBRARY on July 12, 2016

fabrication expertise and preference. The high degree of operational versatility evidenced by the investigations of this research sets the proposed system apart from previous bifurcation-based microscale mass sensing approaches.

Declaration of conflicting interests

The authors declared no potential conflicts of interest with respect to the research, authorship, and/or publication of this article.

Funding

This research was supported in part by the University of Michigan Collegiate Professorship fund.

References

Abu-Salih S and Elata D (2006) Experimental validation of electromechanical buckling. *Journal of Microelectromechanical Systems* 15: 1656–1662.

Aldraihem O and Baz A (2011) Energy harvester with a dynamic magnifier. *Journal of Intelligent Material Systems and Structures* 22: 521–530.

Andò B, Baglio S, Trigona C, et al. (2010) Nonlinear mechanism in MEMS devices for energy harvesting applications. *Journal of Micromechanics and Microengineering* 20: 125020.

Baesens C (1991) Slow sweep through a period-doubling cascade: delayed bifurcations and renormalisation. *Physica D: Nonlinear Phenomena* 53: 319–375.

Berglund N and Gentz B (2000) *Noise-Induced Phenomena in Slow-Fast Dynamical Systems: A Sample-Paths Approach*. London: Springer.

Burgner CB, Turner KL, Miller NJ, et al. (2010) Parameter sweep strategies for sensing using bifurcations in MEMS. In: *Solid-State Sensors, Actuators, and Microsystems Workshop*, Hilton Head Island, SC, 6–10 June, pp. 130–133.

Cleland AN (2005) Thermomechanical noise limits on parametric sensing with nanomechanical resonators. *New Journal of Physics* 7: 235.

Cronin DL (1966) *Response of linear, viscous damped systems to excitations having time-varying frequency*. PhD Thesis, California Institute of Technology, Pasadena, CA.

Ekinci KL, Yang YT and Roukes ML (2004) Ultimate limits to inertial mass sensing based upon nanoelectromechanical systems. *Journal of Applied Physics* 95: 2682–2689.

Elata D and Abu-Salih S (2005) Analysis of a novel method for measuring residual stress in micro-systems. *Journal of Micromechanics and Microengineering* 15: 921–927.

Emery T (2014) Fabrication of bistable MEMS systems for energy harvesting. In: In V, Palacios A and Longhini P (eds) *International Conference on Theory and Applications in Nonlinear Dynamics (ICAND 2012)*. New York: Springer, pp. 123–128.

Gerson Y, Krylov S, Ilic B, et al. (2012) Design considerations of a large-displacement multistable micro actuator with serially connected bistable elements. *Finite Elements in Analysis and Design* 49: 58–69.

Harne RL and Wang KW (2013) Robust sensing methodology for detecting change with bistable circuitry dynamics tailoring. *Applied Physics Letters* 102: 203506.

Harne RL and Wang KW (2014) A bifurcation-based coupled linear-bistable system for microscale mass sensing. *Journal of Sound and Vibration* 333: 2241–2252.

Harne RL, Thota M and Wang KW (2013) Concise and high-fidelity predictive criteria for maximizing performance and robustness of bistable energy harvesters. *Applied Physics Letters* 102: 053903.

Hassanpour PA, Nieva PM and Khajepour A (2011) Stochastic analysis of a novel force sensor based on bifurcation of a micro-structure. *Journal of Sound and Vibration* 330: 5753–5768.

Kovacic I and Brennan MJ (eds) (2011) *The Duffing Equation: Nonlinear Oscillators and their Behaviour*. 1st ed. Chichester: John Wiley & Sons.

Krylov S, Illc BR and Lulinsky S (2011) Bistability of curved microbeams actuated by fringing electrostatic fields. *Nonlinear Dynamics* 66: 403–426.

Kumar V, Boley JW, Yang Y, et al. (2011) Bifurcation-based mass sensing using piezoelectrically-actuated microcantilevers. *Applied Physics Letters* 98: 153510.

Lewis FM (1932) Vibration during acceleration through a critical speed. *Transactions of the American Society of Mechanical Engineers* 54: 253–261.

Li L, Holthoff EL, Shaw LA, et al. (2014) Noise squeezing controlled parametric bifurcation tracking of MIP-coated microbeam MEMS sensor for TNT explosives detection. In: *Proceedings of the 17th US National Congress on Theoretical and Applied Mechanics*, East Lansing, MI, 15–20 June, paper no. D-02-250.

Li M, Tang HX and Roukes ML (2007) Ultra-sensitive NEMS-based cantilevers for sensing, scanned probe and very high-frequency applications. *Nature Nanotechnology* 2: 114–120.

Lifshitz R and Cross MC (2008) Nonlinear dynamics of nanomechanical and micromechanical resonators. In: Schuster HG (ed.) *Reviews of Nonlinear Dynamics and Complexity*, vol. 1. Weinheim: Wiley, pp. 1–52.

Loganathan M and Bristow DA (2014) Bi-harmonic cantilever design for improved measurement sensitivity in tapping-mode atomic force microscopy. *Review of Scientific Instruments* 85: 043703.

Lu CH and Evan-Iwanowski RM (1994) Period doubling bifurcation problems in the softening Duffing oscillator with nonstationary excitation. *Nonlinear Dynamics* 5: 401–420.

Ruzziconi L, Bataineh AM, Younis MI, et al. (2013) Nonlinear dynamics of an electrically actuated imperfect microbeam resonator: experimental investigation and reduced-order modeling. *Journal of Micromechanics and Microengineering* 23: 075012.

Sarioglu AF, Magonov S and Solgaard O (2012) Tapping-mode force spectroscopy using cantilevers with interferometric high-bandwidth force sensors. *Applied Physics Letters* 100: 053109.

Schwab KC and Roukes ML (2005) Putting mechanics into quantum mechanics. *Physics Today* 58: 36–42.

Shaik NH, Reifenberger RG and Raman A (2014) Microcantilevers with embedded accelerometers for dynamic atomic force microscopy. *Applied Physics Letters* 104: 083109.

Downloaded from jim.sagepub.com at OHIO STATE UNIVERSITY LIBRARY on July 12, 2016

Soliman MS and Thompson JMT (1989) Integrity measures quantifying the erosion of smooth and fractal basins of attraction. *Journal of Sound and Vibration* 135: 453–475.

Thundat T, Wachter EA, Sharp SL, et al. (1995) Detection of mercury vapor using resonating microcantilevers. *Applied Physics Letters* 66: 1695–1697.

Turner KL, Burgner C, Yie Z, et al. (2011) Nonlinear dynamics of MEMS systems. *AIP Conference Proceedings* 1339: 111.

Vig JR and Kim Y (1999) Noise in microelectromechanical system resonators. *IEEE Transactions on Ultrasonics, Ferroelectrics, and Frequency Control* 46: 1558–1565.

Wu H, Tang L, Yang Y, et al. (2012) A novel two-degrees-of-freedom piezoelectric energy harvester. *Journal of Intelligent Material Systems and Structures* 24: 357–368.

Wu Z, Harne RL and Wang KW (2014) Energy harvester synthesis via coupled linear-bistable system with multistable dynamics. *Journal of Applied Mechanics: Transactions of the ASME* 81: 061005.

Younis MI and Alsaleem F (2009) Exploration of new concepts for mass detection in electrostatically-actuated structures based on nonlinear phenomena. *Journal of Computational and Nonlinear Dynamics* 4: 021010.

Zhang W and Turner KL (2004) Noise analysis in parametric resonance based mass sensing. In: *Proceedings of IMECE 2004 ASME International Mechanical Engineering Congress and Exposition*, Anaheim, CA, 13–20 November, paper no. IMECE2004-61412.

Zhang W and Turner KL (2005) Application of parametric resonance amplification in a single-crystal silicon micro-oscillator based mass sensor. *Sensors and Actuators A: Physical* 122: 23–30.

Zhang W, Baskaran R and Turner K (2003) Tuning the dynamic behavior of parametric resonance in a micromechanical oscillator. *Applied Physics Letters* 82: 130–132.

Zhou W, Penamalli GP and Zuo L (2012) An efficient vibration energy harvester with a multi-mode dynamic magnifier. *Smart Materials and Structures* 21: 015014.

Zorin AB (1996) Quantum-limited electrometer based on single cooper pair tunneling. *Physical Review Letters* 76: 4408–4411.

Downloaded from jim.sagepub.com at OHIO STATE UNIVERSITY LIBRARY on July 12, 2016